INVESTIGATIONS OF THE GLOW PHASE IN HIGH PRESSURE SPARK DISCHARGES

by

CHI-SUN LEE

B.S., National Taiwan University, 1966

A THESIS SUBMITTED IN PARTIAL FULFILMENT OF

THE REQUIREMENTS FOR THE DEGREE OF

MASTER OF SCIENCE

in the Department

of

PHYSICS

We accept this thesis as conforming to the

required standard

THE UNIVERSITY OF BRITISH COLUMBIA

April, 1971

In presenting this thesis in partial fulfilment of the requirements for an advanced degree at the University of British Columbia, I agree that the Library shall make it freely available for reference and study. I further agree that permission for extensive copying of this thesis for scholarly purposes may be granted by the Head of my Department or by his representatives. It is understood that copying or publication of this thesis for financial gain shall not be allowed without my written permission.

Department of Physics

The University of British Columbia
Vancouver 8, Canada

Date April 29, 1971

ABSTRACT

The glow phase of high pressure spark discharges initiated by the Townsend mechanism of breakdown in hydrogen, nitrogen and carbon dioxide is studied using 16 ohm coaxial cable discharge techniques.

Before the establishment of the spark channel in these low over-voltaged spark discharges, there exist two distinct transition stages, namely, a diffuse glow phase and a filamentary glow-to-channel transition phase. The optical appearance of the diffuse glow is similar to that of a normal d.c. glow discharge. It consists of a negative glow, a Faraday dark space, and a positive column.

From our experimental results it is concluded that for the glow phase the cathode fall voltage and the ratio of the axial potential gradient to the gas pressure in the positive column are fixed for each gas. These values are independent of the impedance of the external circuit and the gas pressure. Comparisons with low pressure d.c. glow discharges indicate further that the cathode fall voltages are in agreement in both types of glow for the gases investigated. In addition, a qualitative discussion about the transition nature of this diffuse glow phase is given on the basis of results obtained from spectroscopic investigations.

TABLE OF CONTENTS

LIST OF TABLES

LIST OF FIGURES

ACKNOWLEDGEMENT

I wish to sincerely thank my supervisor, Dr. J. Meyer, for his advice and help throughout these investigations and the preparation of the thesis. The assistance of the faculty members and students of the plasma physics group is deeply appreciated as well. My special thanks are also due to Mr. D. Stonebridge and Mr. R. P. Haines for their parts in the construction of the apparatus.

CHAPTER 1

INTRODUCTION

1.1 THE HIGH PRESSURE SPARK DISCHARGES

A gas is almost a perfect insulator in its normal state. However if an electric field of sufficient strength is established between two electrodes, the gas can become conducting and the electric current flowing through the gas can range from barely measurable values up to several million amperes or more.

Depending on the duration of current conduction, the discharges are either of a steady state or a transient nature. In spark discharges the transition from the insulating to the highly conducting state of the gas between the electrodes is achieved very rapidly. A short time later, after termination of the current pulse, the initial insulating state is recovered.

Early investigations of high pressure spark discharges have been almost entirely limited to the events immediately following the establishment of the spark channel due to the lack of fast rise-time electrical instruments and sensitive photographic techniques necessary to detect the low light intensities from the earlier stages in the development of these transient discharges. Theories of

the spark channel expansion based on the electrically driven shock wave model have been introduced by Drabkina and Braginskii(1,2) and experimental measurements later have confirmed some of their predictions (3,4).

Due to the recent development of new techniques such as fast rise-time photomultipliers, image converters and image intensifiers, it is possible to study extensively not only the stages following the spark channel formation but also the preceding breakdown process and the initiation of the spark channel itself.

The investigations of the electron avalanches which are responsible for the breakdown of the spark discharges have been carried out, for example, by a research group in Hamburg headed by Prof. H. Raether (5) who some thirty years ago utilized cloud chamber techniques for the earliest studies of the electron avalanches. Most of the features of the initial breakdown processes are now well understood and two breakdown mechanisms can be distinguished: streamer mechanism and Townsend mechanism. Which one the discharge follows depends on the over-voltage applied at the discharge gap.

a. Streamer mechanism: At voltage far in excess of the breakdown voltage across a gap of several centimeter length a spark channel is formed very quickly. Initially an electron avalanche is formed moving toward the anode under the influence

of the high electric field. If the electron density in the avalanche head is amplified beyond a certain value the nature of the avalanche changes, mainly due to the space charge fields, and a streamer of electrons results which bridges the electrodes and produces a pre-channel of fairly high conductivity. The spark channel soon develops and the voltage across the gap collapses very rapidly.

b. Townsend mechanism (generation mechanism): For low to moderate over-voltages and shorter gap distances, a single avalanche cannot cause the electrical breakdown. Instead, successor electrons are produced at the cathode by secondary effects such as positive-ion bombardment and photo-electric effect. Generation avalanches are thus formed and they are responsible for the breakdown. The formative time lag of this type of discharge is much longer as it needs a large number of successor avalanches.

The spark discharges initiated by the Townsend mechanism have been investigated, for example, by Schroder, Doran and Meyer in different gases (6,7,8). It is observed that prior to the complete collapse of the gap voltage, there are transition stages which do not exist in the case of streamer breakdown discharges. At first a diffuse glow-like discharge of low conductivity is formed after breakdown, which exhibits in general a bright negative glow, a Faraday dark space and a uniform positive column. Then a thin filamentary

glow-to-channel transition phase develops and finally a spark channel comes into existence.

Although the breakdown process and the spark channel development have been studied extensively and encouraging success has been achieved, some uncertainty about the contraction process of the diffuse glow still remains unclarified. It seems appropriate therefore, to provide some more information about this glow phase in order to achieve a better understanding of this transient phase.

1.2 OUTLINE OF THE THESIS

It has been shown by Cavenor and Meyer (9) that for the glow phase in hydrogen sparks produced in a 50 ohm coaxial cable discharge arrangement at 500 torr pressure, the gap voltage varies linearly with the electrode distance and the extrapolated zero-length voltage is in agreement with the cathode fall voltage of low pressure d.c. hydrogen glow discharges. To examine whether these characteristics are current dependent or not, a 16 ohm coaxial cable discharge arrangement has been set up and the electrical parameters during the glow phase of hydrogen sparks over a wide range of gas pressures and different gap separations have been measured. The same measurements have been extended to include another two gases — nitrogen and carbon dioxide. The results obtained are presented in Sec. 3.2, together with a description of the

analyzing method which has been used to measure these quantities. These results are discussed in Sec. 5.1 and 5.2 where they are compared with 50 ohm coaxial cable discharge measurements on the one hand and with low pressure d.c. glow discharge measurements on the other.

A monochromator-photomultiplier system has been used to analyze the light emitted during the glow phase from the positive column in nitrogen sparks. The experimental arrangement is briefly outlined in Sec. 4.1. In Sec. 4.2 an estimate of the gas temperature is deduced from the spectral distribution of the nitrogen second positive band spectra. The electron density is evaluated by the methods described in Sec. 4.3. A discussion of the transition nature of the diffuse glow phase based on these results is given in Sec. 5.3.

The following chapter describes the principal and the experimental apparatus of the coaxial cable discharge techniques. Its advantages over the condenser discharge techniques are noted in Sec. 2.1.

1.3 SOME REMARKS ON LOW PRESSURE D.C. GLOW DISCHARGES

Since the transient glow of the spark discharges is quite similar to the d.c. glow discharges in some aspects, the characteristics of the latter will be briefly mentioned here for the purpose of later comparison.

The general optical appearance of the d.c. glow discharges

shows different bright and dark regions, i.e. cathode dark space, negative glow, Faraday dark space, positive column etc. The axial potential distribution is in general not linear except in the positive column, and there the potential gradient is of the order of several volts per centimeter. The anode fall voltage and the voltage drop across the positive column are usually very small compared with the cathode fall voltage. The latter is the potential drop measured from the cathode to the anode end of the Faraday dark space.

For the same gas and the same electrode material the cathode fall voltage is a constant and so is the product of the thickness of cathode fall region and gas pressure (10). The ratio of the axial potential gradient of the positive column to the gas pressure depends very little on the current but is a function of the product of its radius and the gas pressure.

CHAPTER 2

COAXIAL CABLE DISCHARGE TECHNIQUES AND EXPERIMENTAL APPARATUS

2.1 SPARK DISCHARGE TECHNIQUES

In recent years two different techniques have been used to study spark discharges, namely, the condenser discharge techniques and the coaxial cable discharge techniques.

The circuit diagram for the condenser discharges is shown in Fig. 1a. The main disadvantage of this kind of discharge arrangement is that the current rise depends on the external circuit as well as the discharge. As an example, a current oscillogram of such a discharge is illustrated in Fig. 2a.(8)

On the other hand, the only effect of the external circuit in coaxial cable discharges is the limitation of the maximum magnitude of the discharge current. For sufficiently high pressures, for example, the discharge operates almost like an ideal switch and the discharge current rises instaneously (in a fraction of one picosecond) to its maximum value. Therefore in coaxial cable discharges from the measurement of the discharge current it is possible to calculate other important electrical quantities such as the voltage across the gap, the gap resistance and the energy input into the discharge. For this reason we use the coaxial cable discharge techniques

for our investigations rather than the condenser discharge techniques. A typical discharge current oscillogram of coaxial cable spark discharges is sketched in Fig. 2b.

Fig. 1

Circuit Diagrams of the Condenser and the Coaxial Cable Spark Discharges

a. Condenser Spark Discharge

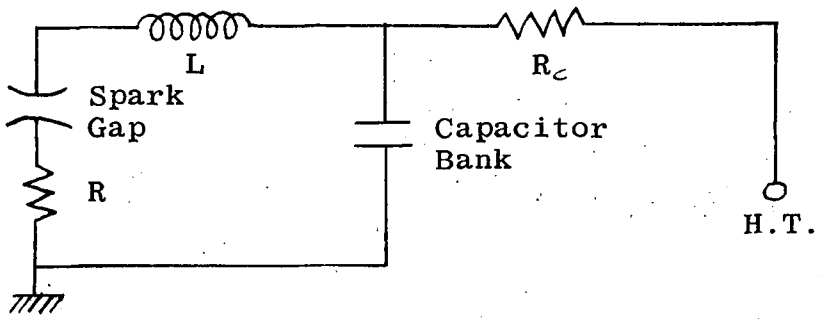

b. Coaxial Cable Spark Discharge

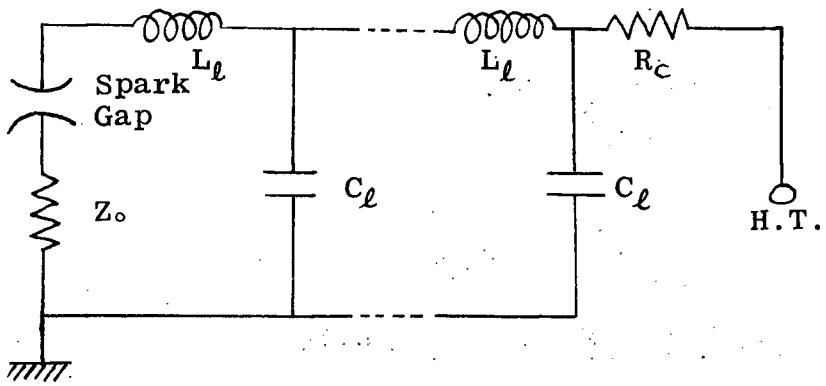

L_ℓ : Inductance per Unit Length of Cable

C_ℓ : Capacitance per Unit Length of Cable

Fig. 2 Current Oscillograms of the Condenser and the Coaxial Cable Spark Discharges under Low Over-Voltage

a. Condenser Spark Discharge

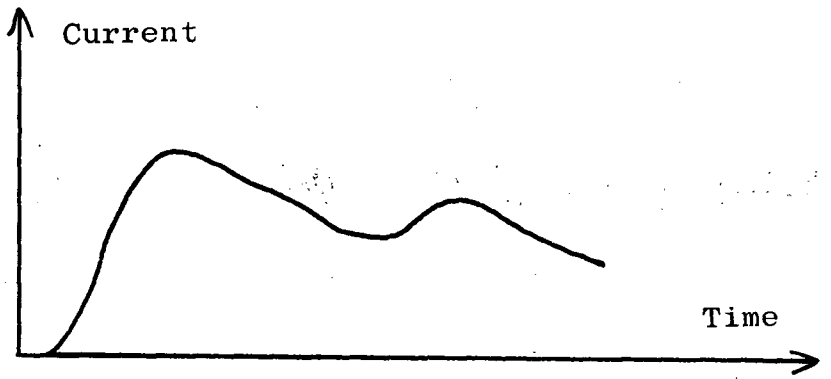

b. Coaxial Cable Spark Discharge

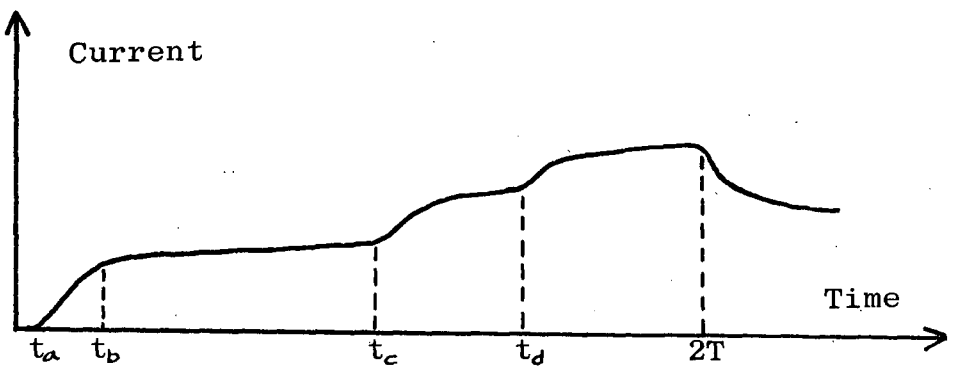

$t_a < t < t_b$ Glow Formation Region
$t_b < t < t_c$ Diffuse Glow Phase
$t_c < t < t_d$ Glow-to-Channel Transition Phase
$t_d < t < 2T$ Spark Channel Stage
T Pulse Transit Time of Pulse-Forming Cable

2.2 THE COAXIAL CABLE DISCHARGE ARRENGEMENT

The principal of the experimental arrangement is illustrated in Fig. 3. A cable of characteristic impedance Z_o (16 ohms in our investigations) is charged through a high resistance R_c and then discharged into a properly terminated cable of the same impedance. The spark chamber is specially designed in order to maintain the same characteristic impedance throughout the whole discharge circuit. Furthermore the chamber can be evacuated and pressurized, and the gap distance of the electrodes can be changed from outside.

During the charging period of the pulse-forming cable, i.e. the period from the instant at which the charging power supply is switched on to the instant at which the discharge starts, there are repeated reflections from both ends since the input end is mismatched and the far end is open-circuited. The voltage E(t) at the far end varies according to:

$$E(t) = U_o\left\{1 - \left[\frac{R_c - Z_o}{R_c + Z_o}\right]^{(t+)/2T}\right\}, \quad \text{when } t = T, 3T, 5T, \ldots$$

$$\cong U_o\left[1 - \exp(-t/CR_c)\right], \quad \text{when } t \gg T$$

where U_o is the charging voltage, R_c the charging resistance, T the total pulse transit time of the cable together with that part of the chamber to which the cable connects, C the total capacitance of this pulse-forming section. When E(t) exceeds the breakdown voltage, breakdown takes place.

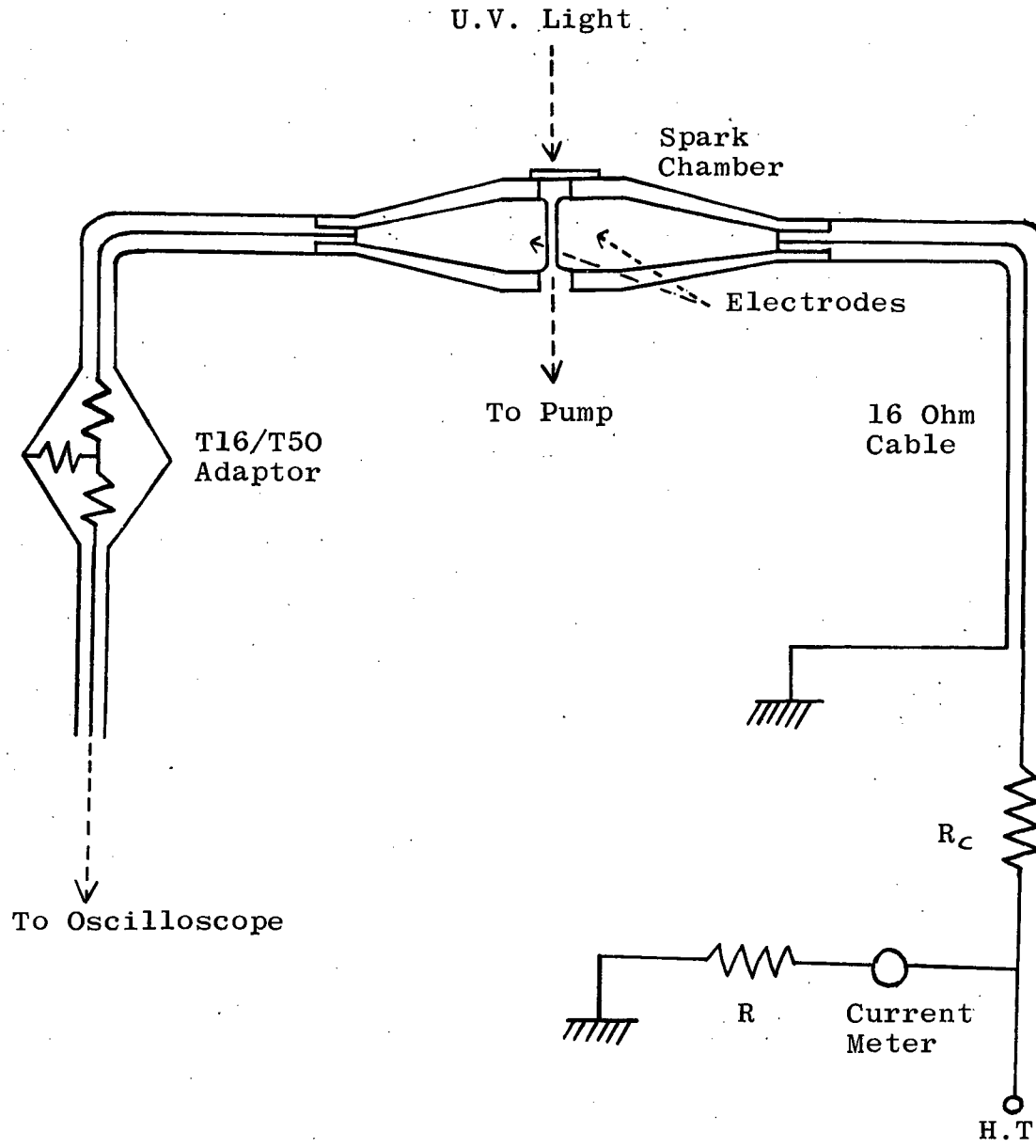

Fig. 3. Coaxial Cable Discharge Arrangement

This causes the collapse of the gap voltage and discharge of the cable, after which the power supply charges up the cable again. Thus we have repeating discharges. The repetition rate can be controlled to some extent by choosing an appropriate charging resistance for cables of different lengths.

If the discharge were to operate as an ideal switch, a rectangular current pulse of height $I_o = U_o/2Z_o$ and duration 2T would be produced. However due to the finite time required to attain high conductivity in the gap, the current rises at a finite rate:

$$I(t) = \frac{U_o}{2Z_o + Z(t)}$$

where $Z(t) = U(t)/I(t)$ is the gap resistance at time t. For a pulse starting at t=O, the above relation holds for $t \leq 2T$. The current pulse is recorded with a Tektronix 519 oscilloscope of rise-time 0.30 nanosecond. The maximum value of 2T of the cables used in our investigations is 197 ns.

Typical current oscillograms are presented in Fig. 4a, 4b, 4c. They all indicate three main stages as mentioned earlier (Fig. 2b). The current pulse for $2T \leq t \leq 4T$ is merely the double reflection of the original current pulse for $O \leq t \leq 2T$. It appears due to to the fact that a finite time is required to attain high conductivity. There are in fact numerous reflections occuring at t = 4T,6T,8T,...., and the

Fig. 4

Current Oscillograms of Spark Discharges

a. Hydrogen	U_o = 2360 V	2T = 197 ns
	P = 700 torr	d = 1.0 mm
b. Nitrogen	U_o = 2780 V	2T = 197 ns
	P = 200 torr	d = 2.0 mm
c. Carbon Dioxide	U_o = 2750 V	2T = 197 ns
	P = 200 torr	d = 1.75 mm
d. Hydrogen	U_o = 2080 V	2T = 95 ns
	P = 1200 torr	d = 0.5 mm

Current Oscillograms of Arrested Glow Discharges

e. Hydrogen	U_o = 2100 V	2T = 95 ns
	P = 600 torr	d = 1.0 mm
f. Nitrogen	U_o = 2070 V	2T = 48 ns
	P = 300 torr	d = 1.0 mm
g. Carbon Dioxide	U_o = 1880 V	2T = 95 ns
	P = 200 torr	d = 1.0 mm

Time-Resolved Light Intensity Variation (λ = 3580 Å) in Nitrogen Transient Glow

h. Time Scale : 2 ns per division

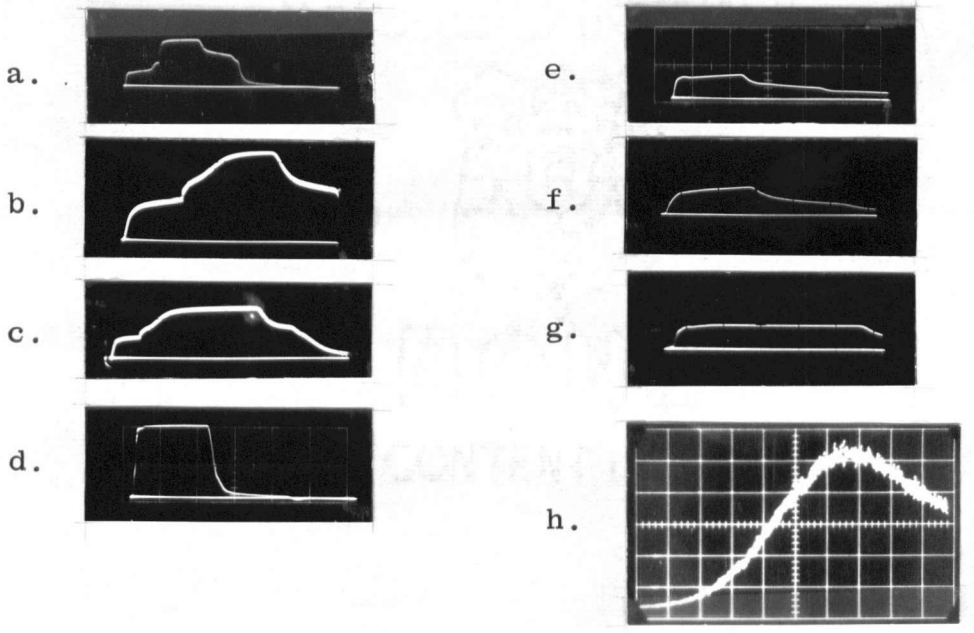

magnitude of these reflections diminishes very rapidly. The rate of rise of the current during the discharge depends on the gas, the pressure and the gap separation. However for any gap distance, the gap resistance falls very quickly after the discharge starts if the gas pressure is high enough (Fig. 4d). This fact will be used later for the calibration of current measurements (Sec. 3.1c).

2.3 EXPERIMENTAL APPARATUS

a. Spark Chamber

The chamber is made of brass and polyethylene, and consists of two separate parts which are joined together by a hollow—cylinder connecter (Fig. 5). There are left-hand and right-hand threads respectively on the inner sides at each end of this connecter. In this way the electrode separation can be changed by rotating the hollow cylinder. The gap distance can be set with an accuracy of 0.015 mm.

In order to prevent signal reflections the geometrical structure of the chamber must satisfy the following equation:

$$Z_o = 138 \left[\frac{1}{k}\right]^{1/2} \log_{10}(D_b / D_a)$$

where k is the dielectric constant of polyethylene, D_b and D_a are inner and outer diameters of the brass coductors as indicated in Fig. 5, and Z_o is 16 ohms here.

Between the brass conductors and the polyethylene tubes

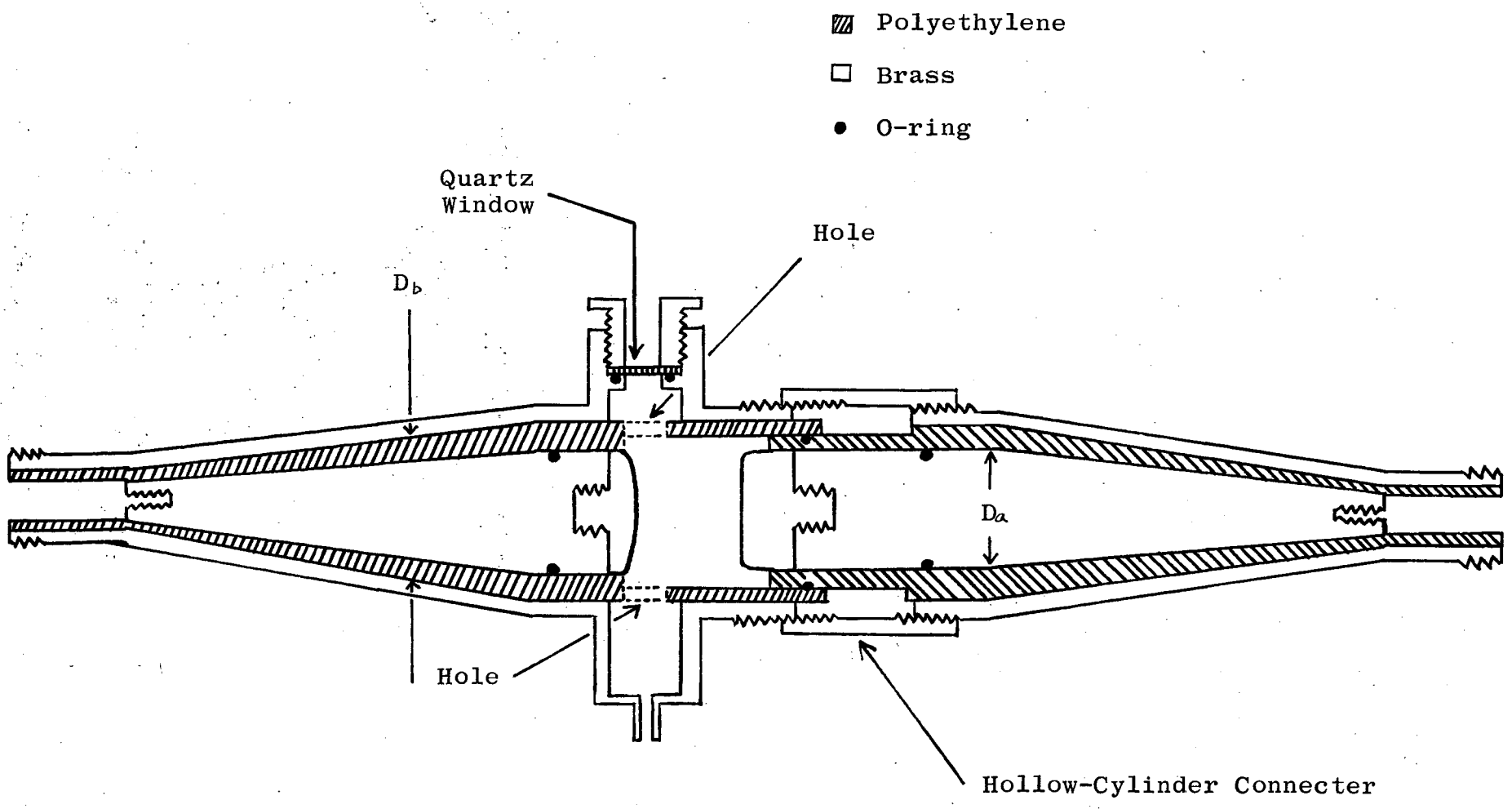

Fig. 5 Spark Chamber

several sets of O-rings are inserted so that the gap is isolated from the atmosphere.

Four holes are drilled through the chamber. One of them serves the outlet for evacuating and pressurizing purposes. The others are fitted with quartz windows. The electrodes can be illuminated through these by ultra-violet light. They also allow the investigation of light emitted from the discharge.

The electrtodes are also made of brass. One of them is plane-surfaced. The other is slightly spherical in order to localize the discharge in the vicinity of the electrodes and yet keep the electric field sufficiently uniform.

b. Impedance-Matched Adaptor

Since the input impedance of the Tek. 519 oscilloscope is 125 ohms, the whole discharge circuit will be mismatched when the oscilloscope is connected directly to the 16 ohm discharge system. A T-type T 16 / T 50 adaptor has been made, which can properly terminate a 16 ohm and a 50 ohm circuits. Another adaptor, e.g. T 50 / T 125 adaptor, is then connected and the discharge current pulses can be properly recorded with the oscilloscope.

The structure of the T 16 /T 50 adaptor is shown in Fig.6. The outer envelope is made of two thin copper cones soldered together and filled with epoxy to provide satisfactory

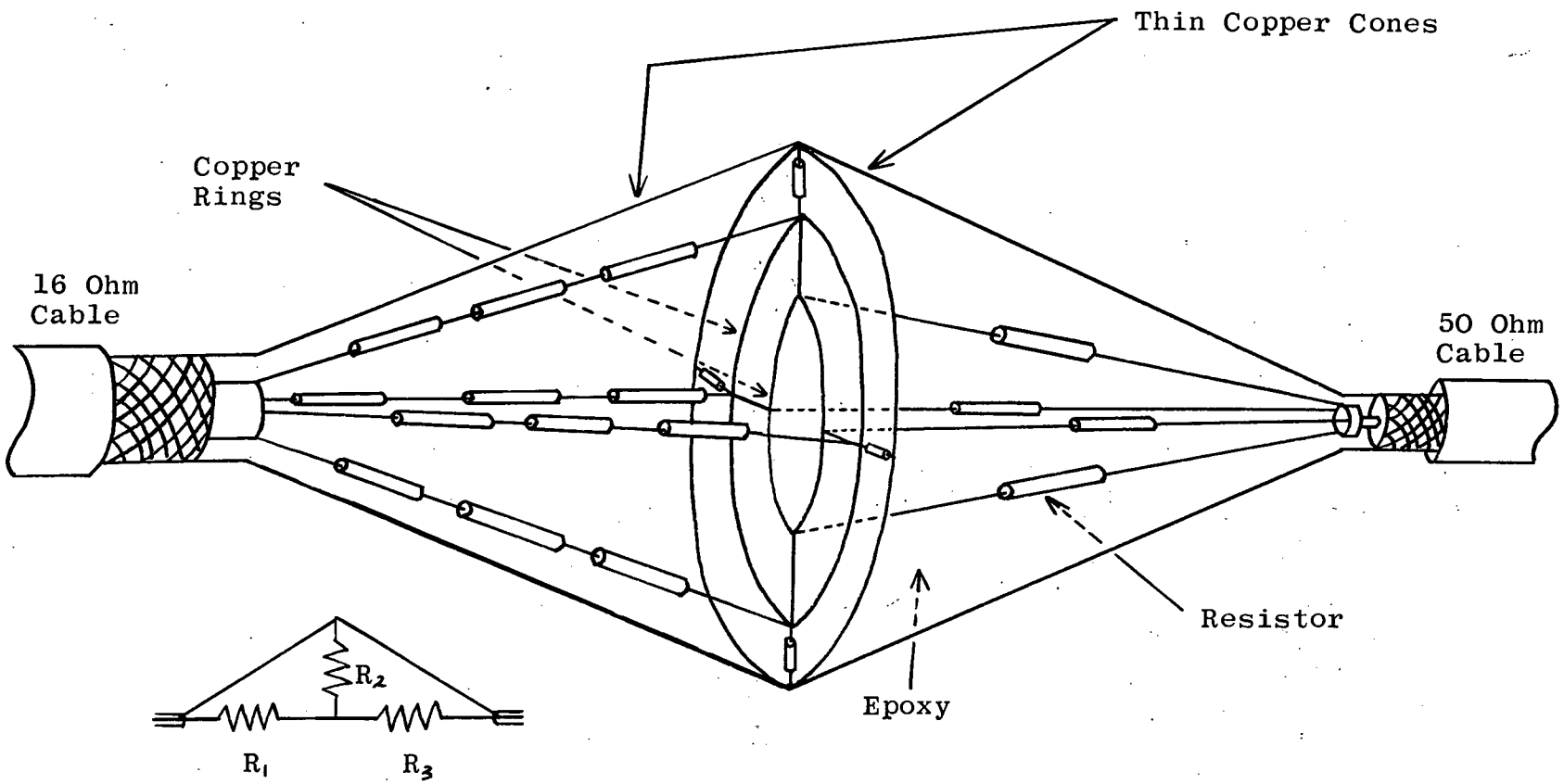

Fig. 6 Impedance-Matched Adaptor

insulation. The values of the resistances R_1, R_2 and R_3, as indicated in the figure, are 11.0, 5.3, and 45.8 ohms respectively. It gives an attenuation factor of 6.1 times from 16 ohm to 50 ohm end. Finally the geometrical structure of the adaptor must also satisfy the equation mentioned in the preceding section, with different Z_o for each end.

CHAPTER 3

ELECTRICAL PARAMETERS

3.1 EXPERIMENTAL AND MEASURING TECHNIQUES

a. Electrode Cleaning Procedures

In order that the discharges occur at consistent breakdown voltage to produce reproducible current pulses, slight over-voltage is applied across the gap. This gives satisfactory discharges triggered by the electrons emitted from the cathode which is illuminated by ultra-violet light. Before resuming experiments, the electrodes are polished and washed in alcohol, and a low pressure glow discharge at about 20 torr in different gases is run between them for about twenty minutes to reduce the absorbed layer of oxygen on the electrode surfaces. These procedures are repeated over and over again to assure the reliability of consistent breakdown.

b. Calibration of the Charging Voltage Measurement

A current meter is connected in series with a resistor and then calibrated to indicate the voltage across this combination. Connecting this in parallel with the power supply, the charging voltage U_o can be measured.

c. Calibration of the Current Measurement

The discharge current traces recorded by the oscilloscope are attenuated by different combinations of attenuators and adaptors. Therefore the attenuation factors of different combinations have to be known in order to calculate the magnitude of the discharge current. It has been mentioned that for sufficiently high gas pressures the discharge current will rise and approach its maximum value $I_o = U_o/2Z_o$ very rapidly but nerer reach it. As illustrated in Fig. 4d, nevertheless, I(2T) + I(4T) is approximately equal to I_o since the currents at 6T, 8T,... are negligibly small. Similar current oscillograms at different pressures and gap separations are recorded and measured. The attenuation factors of different combinations of attenuators and adaptors can thus be determined.

3.2 ANALYSIS OS THE OSCILLOGRAPHIC INVESTIGATIONS

It is observed that the current oscillograms of the spark discharges in the three gases investigated (hydrogen, nitrogen and carbon dioxide) have the similar general characteristic appearance of three distinct stages, if the total pulse transit time T is long enough and the gas pressures are not so high as to cause the spark channel to develop too early. To avoid the appearance of the latter two stages, shorter cables with $2T < t_c$ are used and the discharges are " arrested " in the sense that no subsquent stages can develop and only the glow phase appears.

The feature of these glow phases consists of a negative glow, a Faraday dark space and a positive column. The current oscillograms of the arrested transient glow discharges at different gap separations and gas pressures for all these gases are recorded and three typical ones are presented in Fig. 4e,4f,4g. By measuring the current at the time when the diffuse glow starts to appear for each gas (t_b as indicated in Fig. 2b), and using the relation:

$$U(t) = U_o - 2Z_o I(t) ,$$

the gap voltages at different gas pressures and gap separations can then be calculated. These values obtained for the three gases are plotted against electrode separation in Fig. 7a,7b,7c.

In the normal d.c. glow discharges the axial potential distribution of the positive column can be determined by measuring the gap voltages for various electrode separations while keeping the discharge current constant (10, 11) . However it has been shown by Cavenor and Meyer (9) that for a hydrogen transient glow produced in 50 ohm coaxial cable discharges at 500 torr the distribution can be determined by simply measuring the gap voltages at static breakdown. Even the currents for different gap separations are not the same. In their investigations they first measure the gap voltages at time t_b for different electrode separations under static breakdown conditions (low over-voltage ~1%). Then they perform the same measurements by keeping the currents at time

t_b constant. In order to keep the currents at t_b equal, they must apply appropriate over-voltages as high as 30%. They find that the gap voltages measured under these two different conditions are consistent. Furthermore, framing photos show that the diffuse glow does not change even though the over-voltage has been increased. They therefore conclude that for the current range of their investigations the gap voltage is independent of current. By plotting the gap voltages measured at low over-voltage against gap distance a straight line is obtained. The slope of this line therefore represents the axial potential gradient in the positive column and the extrapolation to zero gap separation results in a potential drop. It has been suggested by Gambling and Edels (11) that this zero-length voltage is equal to the cathode fall voltage.

We assume that the conclusions of Cavenor and Meyer can be extended to higher current range as in the case of our investigations. Then the graphs plotted in Fig. 7 represent the axial potential distributions of the positive column during the diffuse transient glow phase for these gases investigated . The zero-length voltages and the ratios of the axial potential gradient to the gas pressure calculated are listed in the following table.

Table 1

E/P of Positive Column and Cathode Fall Voltage V_c of Hydrogen, Nitrogen, and Carbon Dioxide Glow Phase

Gas	E/P (V/cm-torr)	V_c (V)
Hydrogen	21.7±0.5	220± 5
Nitrogen	36.7±1.0	240± 5
Carbon Dioxide	38.0±1.3	470±10

Fig. 7 Axial Potential Distributions of the Hydrogen, Nitrogen, and Carbon Dioxide Transient Glow

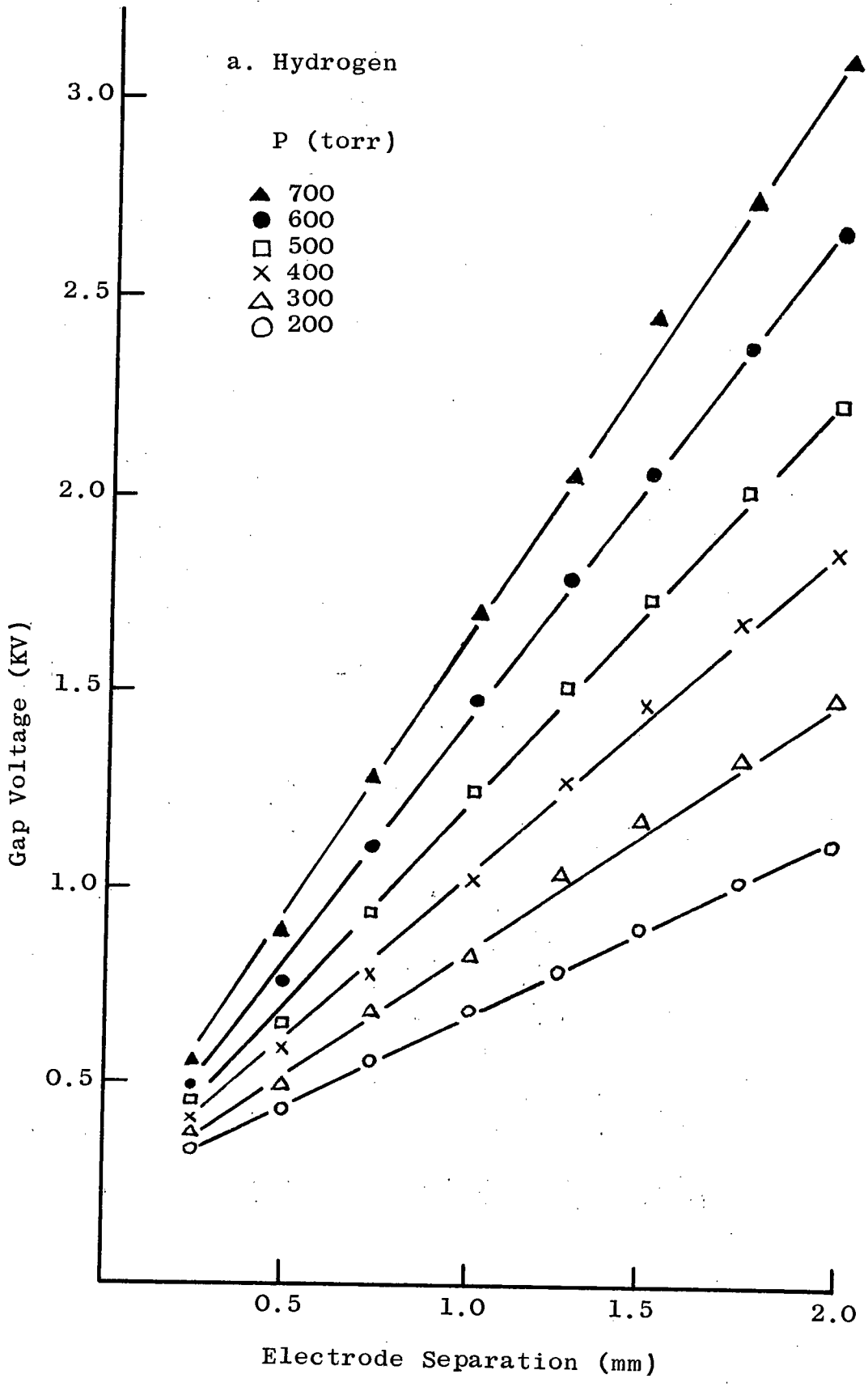

b. Nitrogen

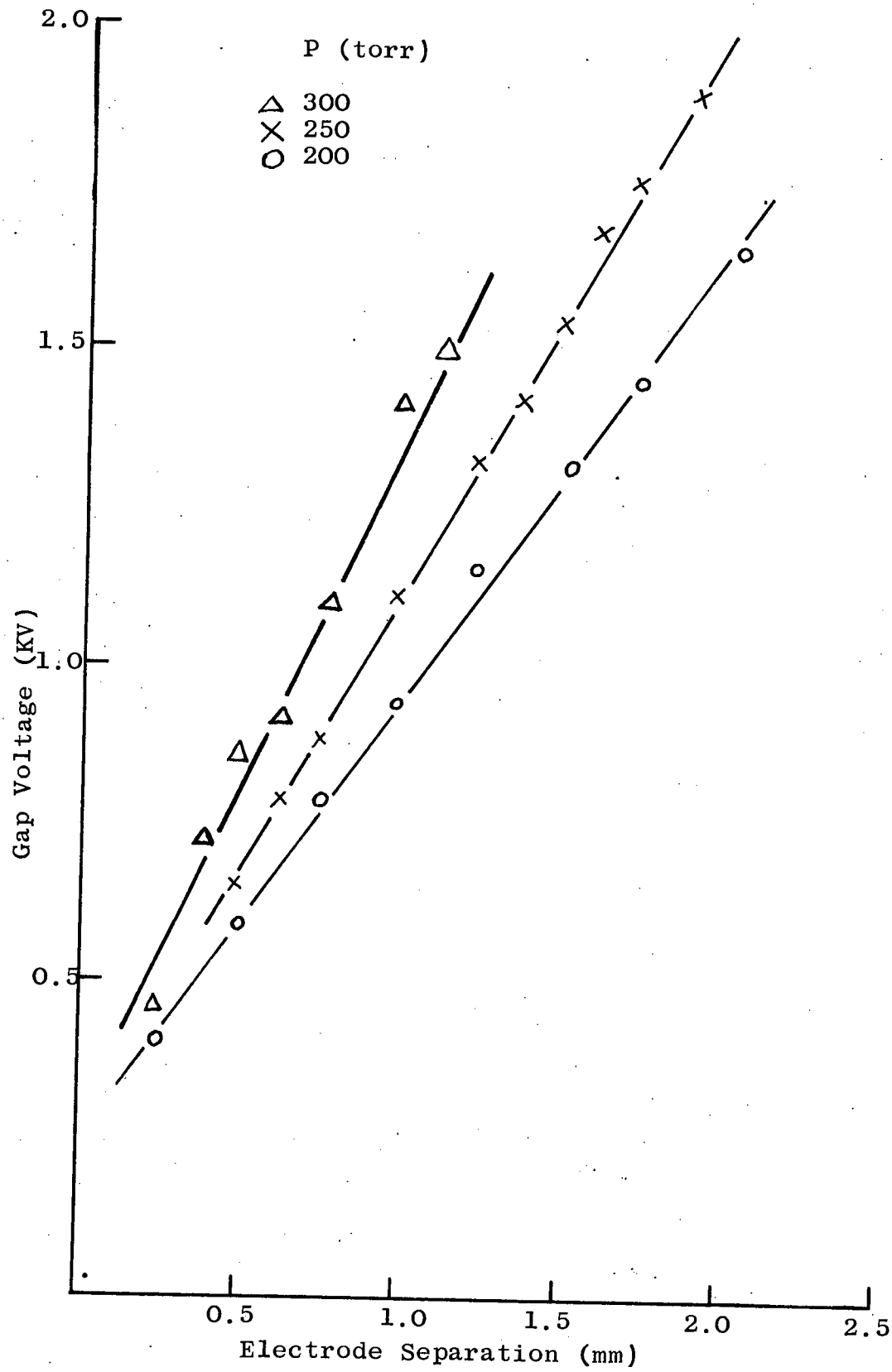
P (torr)
300
250
200
2.0
1.5
1.0
0.5
Gap Voltage (KV)
0.5
1.0
1.5
2.0
2.5
Electrode Separation (mm)

c. Carbon Dioxide

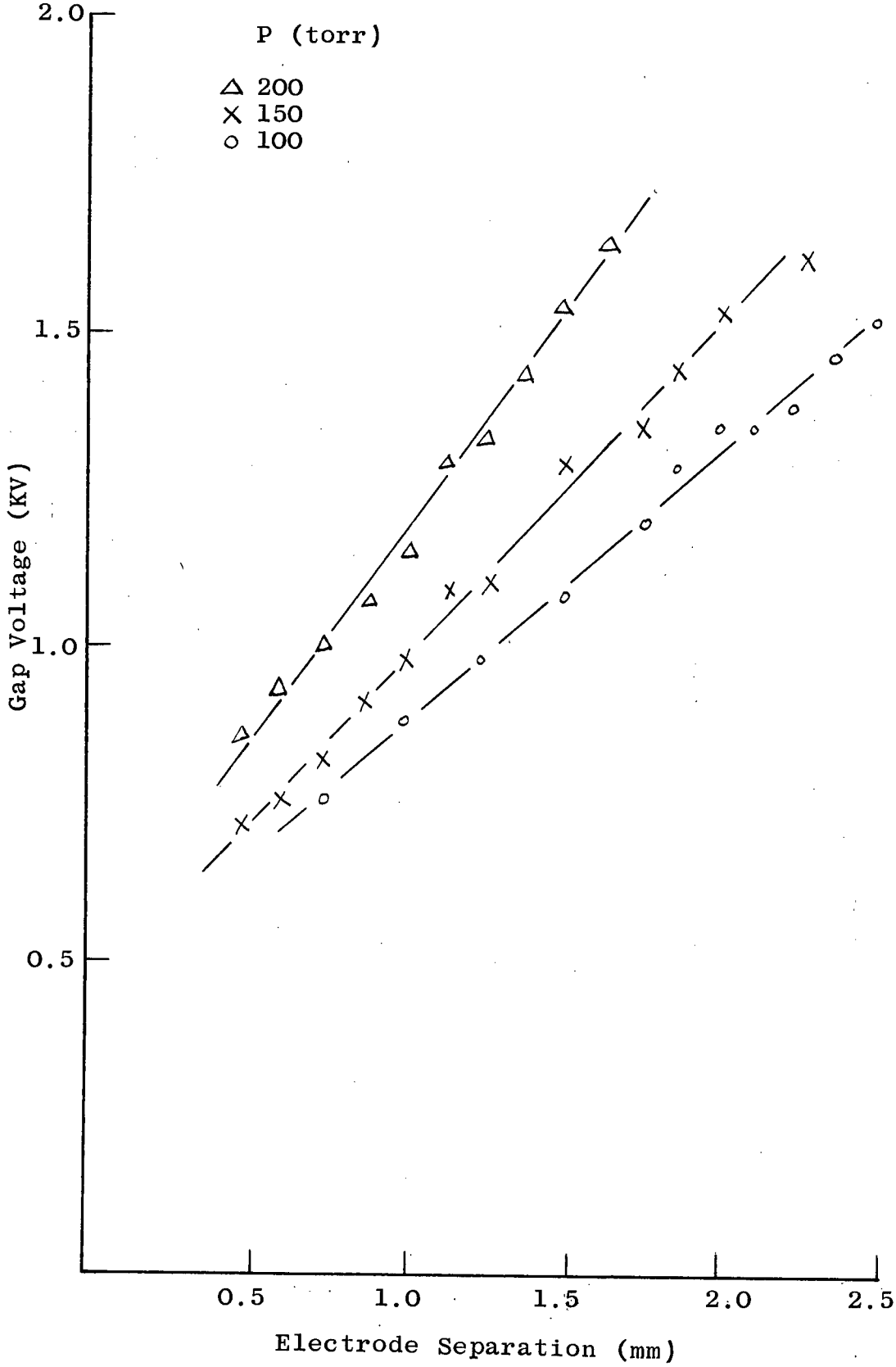

CHAPTER 4

PLASMA PARAMETERS

The gas temperature during the glow phase in nitrogen sparks is estimated from the spectroscopic measurements. The corresponding average electron density is calculated by measuring the magnitude of the discharge current and the diameter of the positive column.

4.1 EXPERIMENTAL ARRANGEMENT FOR TEMPERATURE MEASUREMENT

The block diagram of the experimental arrangement is shown in Fig. 8. The light pulses from the spark discharge column are focused and pass through the entrance slit of a low dispersion monochromator (Bausch and Lomb 50 cm). A R.C.A. type 931-A fast rise-time photomultiplier tube is placed at the exit slit of the monochromator. The light pulses are converted into current pulses which are then fed into the Tek. 1S1 sampling unit of a Tek. 549 storage oscilloscope.

The optical system is aligned with the aid of a He-Ne laser. To calibrate the relative spectral response of the monochromator-photomultiplier system a tungston ribbon lamp is used as the light source. By approximating the lamp as a blackbody, the ratios of the relative spectral radiancy of the light source to the relative photomultiplier response

Fig. 8

Experimental Arrangement for
Spectroscopic Investigations

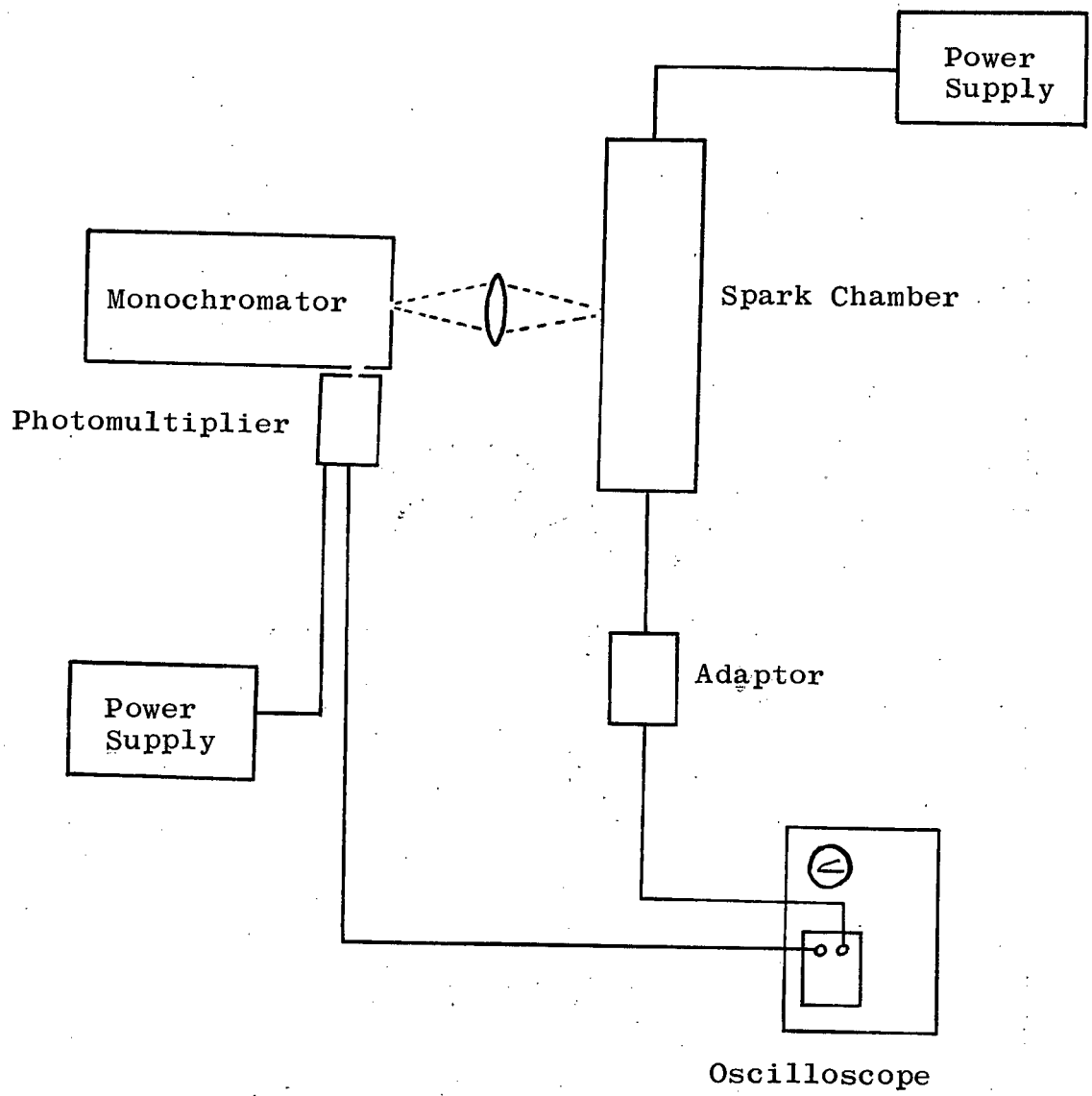

currents for the same wavelengths can be calculated.

4.2 ANALYSIS OF THE SPECTROSCOPIC INVESTIGATIONS

The spark discharges in nitrogen at 200 torr pressure and 1.0 mm gap distance are carried out repeatedly. To assure that the glow discharge is arrested and no subsquent discharges of higher intensity can occur, a very short cable with total pulse transit time T = 5 ns is used. The time-resolved relative intensity variation of the light of different wavelengths emitted from the positive column is indicated by the current trace displayed on the oscilloscope screen. Fig. 4h shows the current oscillogram for $\bar{\lambda}$ = 3580 Å. It is noted that the time duration from the instant the light intensity begins to rise to the instant the intensity reaches its highest value is equal to ten nanoseconds as expected. The relative light intensities for different wavelengths at t = 10 ns are evaluated and plotted in Fig. 9.

The spectra are identified as parts of the second positive band system which usually occurs in the positive column of low pressure nitrogen discharge tubes (12). This particular band system is emitted when nitrogen molecules change from a higher electronic state $C\,^3\pi$ to a lower one $B\,^3\pi$. Each line spectrum corresponds to a vibrational state transition $v \longrightarrow v'$. The observed spectra can be grouped into four bands with $v-v' = 1,2,3,$ and 4.

Fig. 9 Observed Spectra of Nitrogen Second Positive Band System

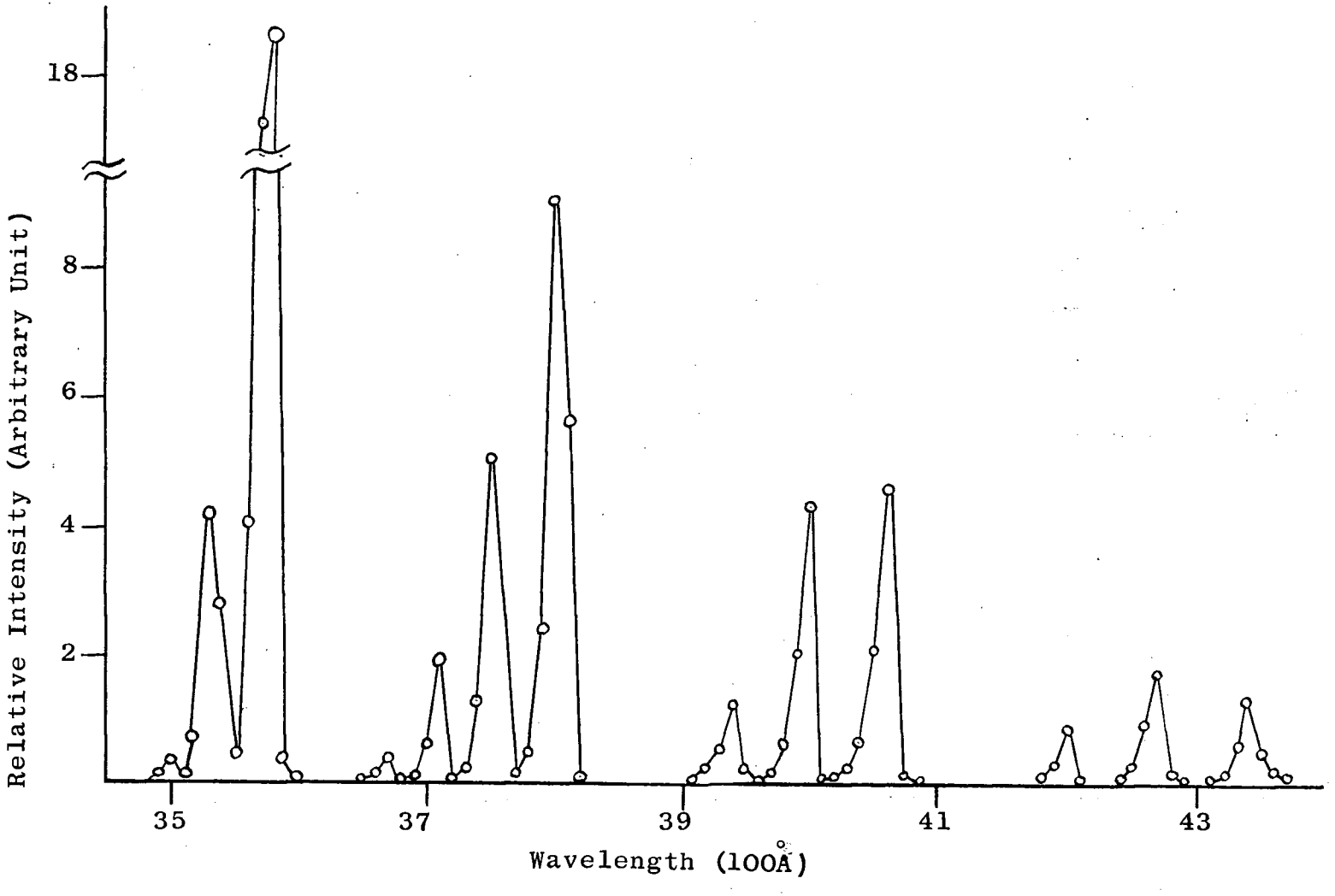

From the theory of diatomic molecular spectra, the light intensity $I(v,v')$ of a $v \longrightarrow v'$ spectral line in an electronic band system is proportional to

$$N(v)\ p(v,v')\left[\lambda(v,v')\right]^{-4}$$

where $N(v)$ is the population of the molecules in v-level, $p(v,v')$ the vibrational transition probability (13). Thus we have:

$$I(v,v')\left[\lambda(v,v')\right]^{4} \propto p(v,v')\left\{\exp\left[-hc\ G(v)/kT\right]\right\}$$

where $G(v)$ is the vibrational energy of the v-level.

The transition probabilities of the nitrogen second positive band system have been calculated by Jarmain and Nicholls (14). Using their results and evaluating the relative light intensity of each observed spectral line, we plot the band strength $\log_e (I\lambda^4/p)$ for each group with the same v-v' and $\log_e \left(\sum_{v'} I\lambda^4 / \sum_{v'} p\right)$ for each v in Fig. 10.

From the nature of these graphs we can conclude that the emission of the second positive band system during the transient glow phase is a process which is dependent upon the statistical equilibrium of the nitrogen molecules in the initial state at one definite temperature. This effective vibrational temperature as calculated from the straight line in Fig. 10b is 2700 ± 100 °K. Unfortunately no information about the effective rotational temperature can be obtained, as the line intensities are too weak tormake possible an

Fig. 10 Band Strengths of Nitrogen Second Positive Band Spectra

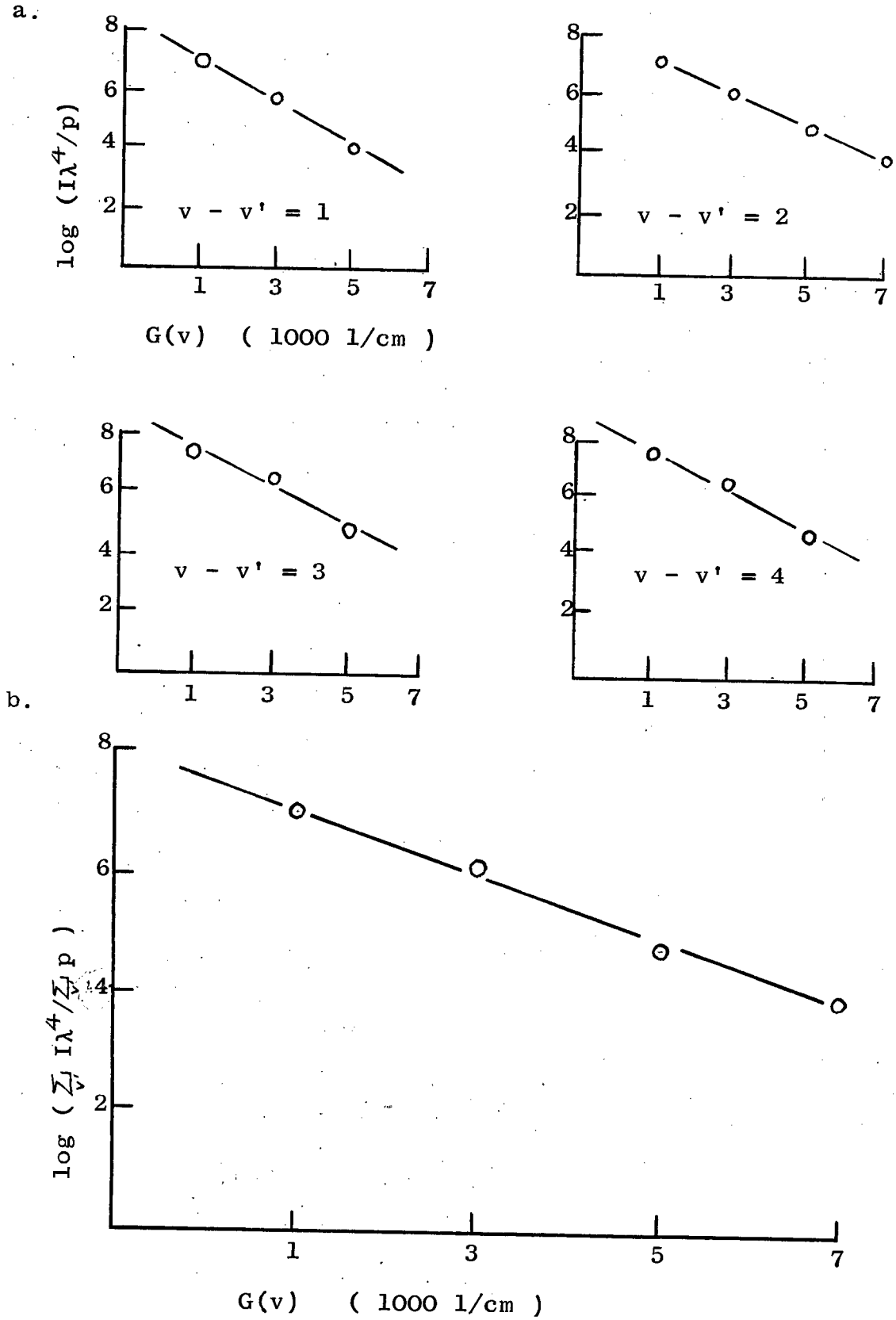

analysis of the rotational structure. However even in non-equilibrium situations the gas temperature does not deviate much from the vibrational temperature and we can therefore conclude that our measurement indicates the gas temperature.

4.3 ELECTRON DENSITY IN THE POSITIVE COLUMN

The discharge current oscillogram of the nitrogen glow is recorded with the Tek. 519 oscilloscope and the current magnitude at $t = 10$ ns is measured. The current density can then be calculated if the cross-sectional area of the discharge column is known. The measurement of the latter is done by two different methods. One method is to take the photographs of the discharge column and then measure the length of the image on the films. The other method is to measure the outermost diameter of the anode spot left by the diffuse glow. The current density calculated is found to be 50 ± 5 A/cm^2.

The current density is given by the expression:

$$J = n_- e_- v_- + n_+ e_+ v_+$$

where n is the number density, e the charge of the charge-carrier, v the drift velocity, with - and + signs referring to electrons and positive ions respectively. For the nitrogen transient glow the value of E/P is 36.7 V/cm-torr as measured in chapter 2. The electron drift velocity at this value is

1.1×10^7 cm/sec and that of the positive ions is only about 1% of v_- (5). Therefore the contribution of the positive ions can be neglected ($n_- \approx n_+$): $J \approx n_- e_- v_-$. The average electron density in the positive column thus evaluated is of the order of 3×10^{13} electrons per cubic centimeter.

CHAPTER 5

DISCUSSIONS AND CONCLUSIONS

5.1 COMPARISON WITH 50 OHM COAXIAL CABLE DISCHARGES

The cathode fall voltage and E/P of the positive column during the hydrogen glow phase as measured in our investigations are 220 V and 21.7 V/cm-torr respectively. The corresponding values obtained by Cavenor and Meyer (9) for a hydrogen glow produced in a 50 ohm coaxial cable discharge arrangement at 500 torr are 220 V and 20 V/cm-torr. Although the discharge current has been increased by more than a factor of two by changing from a 50 to a 16 ohm impedance, it is seen that these values agree well. This fact indicates that during the diffuse glow phase of hydrogen spark discharges initiated by the Townsend mechanism of breakdown, the characteristics as described by constant values of E/P and cathode fall voltage are independent of the impedance of the external circuit.

Our experimental results show that for the glow phase of nitrogen sparks and carbon dioxide sparks, the potential distributions exhibit similar characteristics, i.e. constant E/P and constant cathode fall voltage. Therefore it is reasonable to assume that these quantities are current independent for nitrogen, carbon dioxide and any gas in which the discharge passes through a glow phase.

5.2 COMPARISON WITH LOW PRESSURE D.C. GLOW DISCHARGES

The optical appearance of the diffuse glow is very similar to that of normal d.c. glow discharges. The linear dependence on the gap distance of the axial potential distribution of positive column is another property in common for these two types of glow. Nevertheless, the potential gradient and the gas temperature in the positive column of the former are much higher. In low pressure d.c. glow discharges, these quantities are of the order of a few volts per centimeter and several hundred degrees Kelvin. Furthermore E/P for low pressure d.c. glow discharges is not constant.

Another interesting result is that the cathode fall voltages for both types of glow in the same gas are in agreement. These values for copper and zinc electrodes in hydrogen, nitrogen, and carbon dioxide low pressure d.c. glow discharges are listed in Table 2 (10). Comparison with our results for brass electrodes during the glow phase shows the deviations are less than 13%.

Table 2

Cathode Fall Voltages for Copper and Zinc Electrodes in Hydrogen, Nitrogen, Carbon Dioxide Low Pressure D.C. Glow Discharges

Gas / Electrode	Hydrogen	Nitrogen	Carbon Dioxide
Copper	214	208	460
Zinc	184	216	410

This agreement suggests that the similarity relation holds for the transient glow phase as well, i.e. that the product of the thickness of cathode fall region and gas pressure is a constant for each gas. The product Pd_c , for example, for both copper and zinc electrodes in low pressure hydrogen d.c. glow discharges is 0.8 torr-cm (10). Assuming Pd_c for brass electrodes in hydrogen transient glow is equal to this value, then the average electric field in the cathode fall region $E_c = V_c/d_c$ at different pressures can be calculated from our experimental results. The cathode fall field can also be estimated by another independent method. We assume that during the glow phase the space charge in front of the cathode builds up until it establishes the optimum field for ionizaion. For this purpose we further assume that ion production is predominately the result of electron-molecule ionizing collision processes, defined in terms of α/P where α is the first Townsend ionization coefficient. The maximum " effective " value of α/P has been found to occur at E/P of the order of 300 V/cm-torr (15), and the average cathode field can be estimated. The results are in agreement with the above experimentally determined values.

5.3 THE TRANSITION NATURE OF THE DIFFUSE GLOW PHASE

After the initial breakdown of the gas, the diffuse glow soon appears. Our analysis in the preceding chapter shows that due to the high E/P, only a few nanoseconds later, the gas has

already been heated up to several thousand degrees Kelvin and a high electron density has already developed in the vicinity of the discharge axis. It is then expected that if the discharge is not arrested, the electrical conductivity and the gas temperature will be further increased as the results of related ionizing and heating processes. High pressure and high electron density then build up along the discharge axis and a spark channel soon develops whose expansion can be explained by the theory based on the electrically driven shock wave model.

5.4 CONCLUSIONS

The glow phase of the high pressure spark discharges initiated by the Townsend mechanism of breakdown is quasi-stable in nature. It passes later through a glow-to-channel transition phase and then develops into a highly conducting spark channel. This diffuse glow discharge exhibits a cathode fall region and a uniform positive column across which a considerable potential gradient exists. The characteristics of this transient glow, as described by constant E/P of positive column and by constant cathode fall voltage, are independent of the current limiting impedance. Close similarities between this glow phase and the normal d.c. glow discharges have been noted. These similarities suggest that many of the features of the transient glow, at present difficult to study, may be investigated further by means of experiments carried out on the d.c.

discharges. As our spectroscopic analysis of the nitrogen diffuse glow indicates that the light emission is of molecular origin, which is also the case for hydrogen (9), the results we obtained may be helpful for the study of discharge lasers.

BIBLIOGRAPHY

1. Drabkina, S.I., " J. Exp. Theor. Phys. (USSR) " 1951, 21, p. 473

2. Braginskii, S.I., " Soviet Phys. TEPT " 1958, 7, p. 1068

3. Somerville, J.M. and Williams, J.F., " Proc. Phys. Soc. " 1959, 74, p. 309

4. Andreev, S.T., Vanyukov, M.P. and Kotolov, A.B., " Soviet Phys. Tech. Phys. " 1962, 7, p. 37

5. Raether, H., " Electron Avalanches and Breakdown in Gases " 1964, Butterworths, London

6. Schroder, G.A., " Proc. 7th Int. Conf. on Phen. in Ionized Gases, Belgrad " 1966, I, p.606

7. Doran, A.A. and Meyer, J., " Brit. J. Appl. Phys. " 1967, 18, p. 793

8. Doran, A.A., " Z. Phys. " 1968, 208, p. 427

9. Cavenor, M.C. and Meyer, J., " Aust. J. Phys. " 1969, 22, p. 155

10. Cobine, J.D., " Gaseous Conductors " 1941, McGraw-Hill, New York

11. Gambling, W.A. and Edels, H., " Brit. J. Appl. Phys. " 1954, 5, p. 36

12. Pearse, R.W.B. and Gaydon, A.G., " The Identification of Molecular Spectra " 1963, Chapman and Hall, London

13. Herzberg, G., " Molecular Spectra and Molecular Structure, I. Spectra of Diatomic Molecules " 1950, Van Norstrand, New York

14. Jarmain, W.R. and Nicholls, R.W. " Can. J. Phys." 1954, 32, p. 201

15. Haydon, S.C. and Stock, H.M.P., " Aus. J. Phys. " 1966, 19, p. 795